

DETECTION OF THE INTERSTELLAR NH₂ RADICAL

EWINE F. VAN DISHOECK AND DAVID J. JANSEN

Sterrewacht Leiden, Postbus 9513, NL-2300 RA Leiden, The Netherlands

AND

PETER SCHILKE AND T. G. PHILLIPS

Division of Physics, Mathematics, and Astronomy, California Institute of Technology 320-47, Pasadena, CA 91125

Received 1993 July 12; accepted 1993 August 4

ABSTRACT

The NH₂ radical has been detected for the first time in interstellar clouds. Using the Caltech Submillimeter Observatory, five features containing 15 lines of NH₂ have been observed in absorption toward Sgr B2(N) and Sgr B2(M). The NH₂ is located in a low-density envelope in front of the dense, hot cores seen in emission lines of other molecules. It is not detected in the hot cores themselves. We infer a NH₂ column density of $5 \times 10^{15} \text{ cm}^{-2}$, a fractional abundance relative to H₂ of $(1-3) \times 10^{-8}$, and a total NH₂/NH₃ column density ratio in the envelope of 0.5. In addition to gas-phase ion-molecule chemistry, shock chemistry is likely to be important. In the dense, hot cores of Sgr B2(M) and (N) the NH₂/NH₃ ratio is substantially lower, in agreement with significant grain-surface formation of NH₃ but not of NH₂.

Subject headings: ISM: abundances — ISM: individual: Sagittarius B2 — ISM: molecules — line: identification — molecular processes — radio lines: ISM

1. INTRODUCTION

Simple hydride molecules are the building blocks of the interstellar chemistry networks (Herbst & Klemperer 1973; Dalgarno & Black 1976), but their detection in the dense interstellar medium is made difficult by the fact that the lowest rotational transitions occur at submillimeter wavelengths, where the atmospheric transmission is often poor. In spite of this, several fundamental transitions have been observed, e.g., of HCl (Blake, Keene, & Phillips 1985), NH₃ (Keene, Blake, & Phillips 1983), HDO (Schulz et al. 1991), OH (Storey, Watson, & Townes 1981) and H₂S (Thaddeus et al. 1972). One of the simplest polyatomic hydrides is the NH₂ radical for which the $1_{10-1_{01}}$ transition lies at 460–470 GHz, a region which is accessible from the ground. We report here the results of the first successful search using the Caltech Submillimeter Observatory (CSO).

The spectrum of NH₂ is typical of that of an asymmetric rotor but differs from the spectrum of, e.g., H₂O in that NH₂ has a 2B_1 electronic ground state with a net unpaired electronic spin of $\frac{1}{2}$. Each rotational level, $N_{K_a K_c}$, is therefore split into two levels with $J = N + \frac{1}{2}$ and $J = N - \frac{1}{2}$. Because the two hydrogen nuclei are identical, ortho and para modifications occur in which $K_a + K_c = \text{even or odd}$, respectively. Hyperfine interactions involving the ^{14}N nuclear spin further split all NH₂ levels, and additional splittings occur due to the net proton spin in the case of ortho-NH₂ (Burkholder, Howard, & McKellar 1988). The frequencies of most lines within the $1_{10-1_{01}}$ transition of para-NH₂ have been accurately measured by Charo et al. (1981), although they give only the strongest components. The complete list of frequencies and strengths of the observed lines is given in Table 1, where the line strengths were calculated using the model of Cook & De Lucia (1971).

Chemically, the NH₂ radical is of considerable interest for testing the production pathways of nitrogen-bearing molecules. The NH₂ chemistry is directly related to that of the widely observed NH₃ molecule. The ion-molecule reactions

involved in the formation of NH₃ are notoriously complex (Le Bourlot 1991), and synthesis of the molecule on the surfaces of interstellar grains may be significant in some regions (Jacq et al. 1990). This conclusion also applies to diffuse clouds, where the NH radical has recently been observed through absorption lines at ultraviolet wavelengths (Meyer & Roth 1991). The detection of interstellar NH₂ provides an important missing link in the chemistry of these simple hydrides and may help to distinguish between the various scenarios.

2. RESULTS

The spectra obtained for the three components at 461.4, 462.4, and 469.4 GHz toward Sgr B2(M) and (N) are presented in Figure 1. The half-power beamwidth of the CSO at these frequencies is 16", and the main beam efficiency was measured to be 50% by observations of Jupiter. Clear absorption features are visible at all expected positions of the NH₂ lines. Local oscillator shifts confirmed the sideband identification: there is no doubt that all 5 blends can be ascribed to NH₂, containing 15 lines in total.

Since the absolute continuum level is rather uncertain in our spectra due to the slow beam-switching technique making the system sensitive to atmospheric variations, we have performed an optical depth fit based on the intensity ratios of the various hyperfine components in the 461 and 462 GHz lines. This is a standard procedure for determining NH₃ optical depths (Pauls et al. 1983). The results for Sgr B2(M) are displayed in Table 1. A single best-fit velocity of $66 \pm 2 \text{ km s}^{-1}$ is found. Toward Sgr B2(N), the fitting is more difficult because of the presence of two velocity components at 63 and 81 km s⁻¹ (see, e.g., Martín-Pintado et al. 1990). This second component at 81 km s⁻¹ is not obvious in the 462 GHz spectrum (apart from an increase to the line width) but shows up as red wings on the 461 and 469 GHz lines. If the velocities of the two components are fixed at 63 and 81 km s⁻¹, the fitting procedure gives $\tau = 2.3 \pm 0.7$ and $\tau = 1.0 \pm 0.3$ for the strongest hyperfine line, with $\Delta V = 16.4 \pm 2.3$ and $12.8 \pm 1.4 \text{ km s}^{-1}$, respectively.

TABLE 1
OBSERVED OPTICAL DEPTHS OF NH₂ LINES TOWARD Sgr B2(M)

Component $J' - J''$	Line $F' - F''$	Frequency (GHz)	Relative intensity ^a	Optical depth τ
$\frac{3}{2} - \frac{3}{2}$	$5 - 5$	462.43351	10.0	3.8 ± 1^b
	$5 - 4$	462.46366	1.90	<i>c</i>
	$4 - 4$	462.42542	1.90	<i>c</i>
	$4 - 3$	462.45558	4.27	<i>c</i>
	$3 - 3$	462.47358	1.76	<i>c</i>
	$3 - 2$	462.44904	1.76	<i>c</i>
$\frac{1}{2} - \frac{1}{2}$	$2 - 2$	462.46702	2.20	<i>c</i>
	$3 - 2$	469.44062	3.54	1.2 ± 0.3
	$3 - 1$	469.38337	2.83	1.2 ± 0.3
	$2 - 1$	469.36612	2.83	
	$1 - 1$	469.30888	0.35	<0.2
$\frac{3}{2} - \frac{1}{2}$	$5 - 3$	461.46503	2.35	1.1 ± 0.3
	$4 - 3$	461.45695	0.70	
	$4 - 2$	461.45039	0.09	
	$3 - 1$	461.39972	0.87	1.0 ± 0.3
$2 - 1$	461.39316	0.70		

^a Relative intensities obtained from a first-order model and scaled such that the strongest line at 462.43351 has an intensity of 10.

^b Fitting procedure gives $V_{\text{LSR}} = 66 \pm 2 \text{ km s}^{-1}$ and $\Delta V = 13.8 \pm 1.2 \text{ km s}^{-1}$.

^c Blended with strongest line; optical depths not independently determined.

The continuum levels determined from the optical depths derived above are 8 K for Sgr B2(M) and 9.5 K for Sgr B2(N). For comparison, the temperatures derived by interpolating the continuum observations of Goldsmith et al. (1990) measured with a similar beam are 17.6 K and 19.1 K, respectively. In giant molecular clouds (GMCs) it is often the case that hetero-

dine and bolometer results differ by a factor of 2 owing to the contribution of the many molecular lines to the wideband flux (Sutton et al. 1985).

The 469 GHz lines lie close to an atmospheric feature and do not have high enough signal-to-noise ratio to be fitted with the hyperfine method. However, their optical depths can be deter-

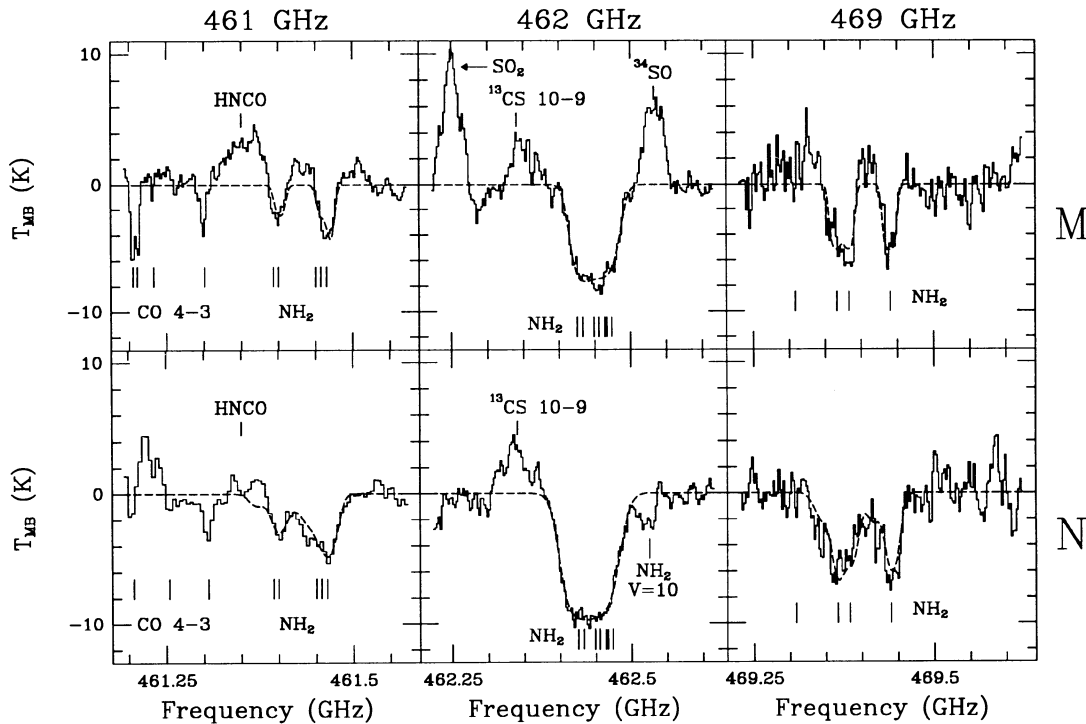


FIG. 1.—Spectra of NH₂ at 461, 462, and 469 GHz toward Sgr B2(M) (top), $\alpha_{1950} = 17^{\text{h}}44^{\text{m}}10^{\text{s}}.6$, $\delta_{1950} = -28^{\circ}22'05''$, and Sgr B2(N) (bottom), $\alpha_{1950} = 17^{\text{h}}44^{\text{m}}10^{\text{s}}.6$, $\delta_{1950} = -28^{\circ}21'20''$. The dashed lines are the hyperfine fits to the NH₂ lines. In the 461 GHz spectra, some CO 4–3 absorption features in spiral arm clouds are seen as well. NH₂ absorption at $V_{\text{LSR}} = 10 \text{ km s}^{-1}$ is indicated in the 462 GHz spectrum toward Sgr B2(N).

mined using the continuum levels inferred from the other lines. The results are included in Table 1 and are consistent with the other lines.

The 462 GHz line of NH₂ was mapped in Sgr B2 over a 6×10 point grid with 15" spacing (Fig. 2). The sources Sgr B2(N) (*top*) and Sgr B2(M) (*bottom*) are clearly seen in absorption, but no significant absorption or emission is seen at other positions. Comparison with the continuum maps of Goldsmith et al. (1990) shows that the features seen in NH₂ basically trace the dust continuum, suggesting that there is no major variation of the NH₂ abundance over the map range. NH₂ thus seems to be a fairly widespread molecule which happens to be only easily observable in absorption towards strong continuum sources, for reasons of excitation.

3. ANALYSIS

The best studied parts of the Sgr B2 molecular cloud are the Sgr B2(N) and (M) hot ($T_{\text{kin}} \approx 150\text{--}200$ K) and dense [$n(\text{H}_2) > 10^6 \text{ cm}^{-3}$] cores, which show strong submillimeter line (Sutton et al. 1991) and continuum emission due to dust (Goldsmith et al. 1990). Located in front of them is a cool, more extended low-density envelope from which lines of molecules such as NH₃, H₂CO, SiO, CS, HCN, CN, and CH₃OH have been observed in absorption at $V_{\text{LSR}} \approx 66 \text{ km s}^{-1}$ against Sgr B2(M) and at 63 and 81 km s⁻¹ toward Sgr B2(N) (e.g., Martin-

Pintado et al. 1990). The widths of these lines are similar to those we see for NH₂, suggesting that this radical arises in the same region. There is some evidence for weak NH₂ absorption at $V_{\text{LSR}} \approx 0\text{--}20 \text{ km s}^{-1}$ toward Sgr B2(N) with $\tau \approx 0.1\text{--}0.3$. The total column density of the Sgr B2 cool envelope has been estimated from C¹⁸O emission (Lis & Goldsmith 1989) to be about $N(\text{H}_2) \approx 2 \times 10^{23} \text{ cm}^{-2}$ for Sgr B2(M) and the Sgr B2(N) 63 km s⁻¹ component, and slightly less for the 81 km s⁻¹ component. The density has been determined to be between 5×10^3 and $1 \times 10^5 \text{ cm}^{-3}$ and the temperature to be around 20 K (Lis & Goldsmith 1991).

Recent observations of highly excited NH₃ absorption lines suggest the presence of a shock in the low density envelope of Sgr B2 (Wilson et al. 1982; Wilson, private communication). The NH₃ observations indicate $T_{\text{kin}} \approx 900$ K, $n(\text{H}_2) < 10^4 \text{ cm}^{-3}$ and $N(\text{NH}_3) \approx 10^{16} \text{ cm}^{-2}$. If the abundance of NH₃ were standard, about 10^{-7} , this would result in a total H₂ column density of 10^{23} cm^{-2} . Such a high column density of very hot gas would not escape observation in the various CO isotopes even at low densities, but it is not found. We have to conclude that the NH₃ abundance is probably enhanced by a few orders of magnitude in the shock and that the H₂ column density of the shocked region can be only a fraction of the total column density in the envelope. On the other hand, the NH₃ column density in the envelope is dominated by the shocked component.

A lower limit to the para-NH₂ column density can be obtained from the observed optical depths assuming that all of the population is in the lowest 1₀₁ level. The results, presented in Table 1, imply $N(J'' = 3/2) \approx 7.2 \times 10^{14} \text{ cm}^{-2}$ and $N(J'' = 1/2) \approx 4.0 \times 10^{14} \text{ cm}^{-2}$ toward Sgr B2(M), leading to $N(\text{para-NH}_2) \geq (1.1 \pm 0.3) \times 10^{15} \text{ cm}^{-2}$. If the ortho/para ratio is 3, a total NH₂ column density of at least $4.4 \times 10^{15} \text{ cm}^{-2}$ is found. For the Sgr B2(N) 63 and 81 km s⁻¹ clouds we find $3.2 \times 10^{15} \text{ cm}^{-2}$ and $1.1 \times 10^{15} \text{ cm}^{-2}$, respectively.

In order to better constrain the NH₂ column density, an excitation model was set up for both ortho- and para-NH₂ including the spin-rotation splittings but not the hyperfine splittings. The Einstein A coefficients were calculated using a dipole moment of 1.83 D (Millar et al. 1991) and rotational line-strength factors provided by K. Kawaguchi (private communication). A collisional rate coefficient of $2 \times 10^{-11} \text{ cm}^3 \text{ s}^{-1}$ was adopted for the $N = 1\text{--}0$ transitions, and all other rate coefficients were assumed to scale with the radiative line strengths. The radiative transfer was treated in an escape probability formalism.

The intense far-infrared radiation from warm dust significantly affects the excitation of hydrides, as has been demonstrated for H₃O⁺ in Sgr B2 by Phillips, van Dishoeck, & Keene (1992). However, even if dust radiation is included with $T_d \approx 40\text{--}70$ K and a total dust column corresponding to $A_V \approx 100\text{--}300$ mag, the fraction of para-NH₂ molecules in the lowest levels is still $\geq 85\%$. The best estimate of the total para-NH₂ column density from the models is therefore $(1.3 \pm 0.3) \times 10^{15} \text{ cm}^{-2}$ for Sgr B2(M), corresponding to a total ortho- + para-NH₂ column density of $(5.2 \pm 1.2) \times 10^{15} \text{ cm}^{-2}$. Toward Sgr B2(N), we find $(3.8 \pm 1.0) \times 10^{15} \text{ cm}^{-2}$ and $(1.3 \pm 0.5) \times 10^{15} \text{ cm}^{-2}$ for the 63 and 81 km s⁻¹ clouds, respectively. The corresponding NH₂ abundance is $(1\text{--}3) \times 10^{-8}$. For comparison, the total NH₃ column density in the cool and shocked components of the envelope, as derived from absorption in the inversion lines, is 10^{16} cm^{-2} . The resulting overall NH₂/NH₃ ratio is 0.5, if NH₂ is similarly distributed as NH₃.

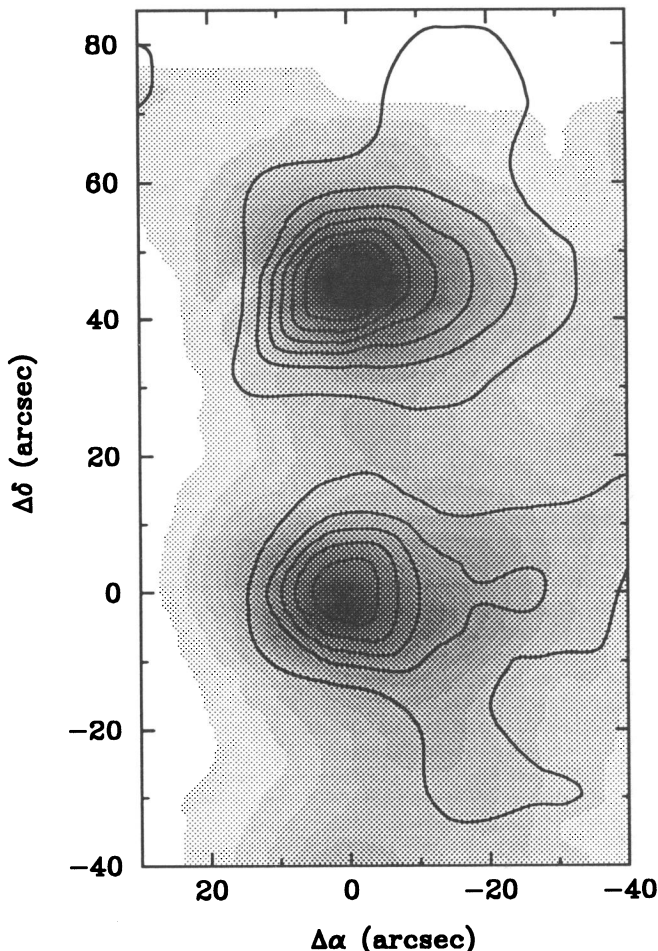


FIG. 2.—Comparison of 800 μm continuum data (gray scale), taken from Goldsmith et al. 1990, and integrated NH₂ intensity (contours). The contour levels for NH₂ are -300 to -50 km s^{-1} in steps of 50 K km s^{-1} . The map center is Sgr B2(M) at $\alpha_{1950} = 17^{\text{h}}44^{\text{m}}10^{\text{s}}.6$; $\delta_{1950} = -28^{\circ}22'05''$.

Why is no NH_2 emission seen from the hot dense cores Sgr B2(N) and (M) themselves? Ammonia emission in non-metastable lines suggests high NH_3 abundances of order 10^{-5} (e.g., Vogel, Genzel, & Palmer 1987). The NH_2 excitation calculations show that for $T_{\text{kin}} \approx 100\text{--}200$ K, $n(\text{H}_2) \approx 10^6\text{--}10^7$ cm^{-3} , $T_d \approx 150\text{--}250$ K, and $A_V \approx 1000$ mag or larger, the $1_{10}\text{--}1_{01}$ lines of para- NH_2 will occur weakly in absorption against the strong dust continuum. Higher excitation lines such as the $3_{13}\text{--}2_{20}$ line of ortho- NH_2 at 229 GHz should be in emission. The failure to detect any emission at 229 GHz at the level $T_{\text{MB}} \leq 0.1$ K implies $N(\text{ortho-}\text{NH}_2) < 6 \times 10^{14}$ cm^{-2} in the CSO 32" beam, if the high-density material covers that beam. If the source size is as small as 5", the upper limit is increased to 2×10^{16} cm^{-2} . This corresponds to an NH_2 abundance of $< 5 \times 10^{-9}$ and $< 2 \times 10^{-8}$ in Sgr B2(N) and (M), respectively, if column densities of 5×10^{24} and 1×10^{24} cm^{-2} are adopted for the two cores (Martín-Pintado et al. 1990). Thus, the NH_2/NH_3 abundance ratio is less than 10^{-3} in the cores, suggesting a very different nitrogen chemistry from that in the envelope.

The NH_2 optical depth for the cloud at $V_{\text{LSR}} \approx 10$ km s^{-1} is at least one order of magnitude lower than that for the Sgr B2 envelope. If all of the absorption arises in a single cloud with $\Delta V \approx 15$ km s^{-1} , $N(\text{NH}_2) \approx (3 \pm 1) \times 10^{14}$ cm^{-2} is found. The total hydrogen column density for this component is uncertain but is of order $N(\text{H}_2) \approx (1\text{--}2) \times 10^{22}$ cm^{-2} if standard CS, HCO^+ , and HCN abundances are assumed (Greaves et al. 1992). Thus, the NH_2 abundance appears similar to that in the Sgr B2 envelope. The NH_3 column density also seems to be roughly 10 times lower than that in the 63 km s^{-1} component (Gardner, Boes, & Winnewisser 1988), about 4×10^{14} cm^{-2} . Therefore, the NH_2/NH_3 ratio in this cloud is about 0.75.

4. CHEMISTRY

In the standard gas-phase ion-molecule chemistry scheme, the formation of nitrogen hydrides is initiated by the reaction $\text{N}^+ + \text{H}_2 \rightarrow \text{NH}^+ + \text{H}$, which has a small energy barrier for reaction with para- H_2 but not with ortho- H_2 (Le Boulrot 1991). A series of hydrogen abstraction reactions subsequently leads to NH_3^+ and NH_4^+ which can recombine with electrons to form NH_2 and NH_3 . At steady state, typical dark cloud model NH_2 abundances are $(1\text{--}5) \times 10^{-8}$, and the NH_2/NH_3 ratio is found to range from 0.3–1.5 for a wide variety of assumptions (Millar et al. 1991; Langer & Graedel 1989). If

photodissociation of NH_3 is included, the model NH_2/NH_3 ratio increases by factors of a few. Both the observed ratio in the envelope ($\text{NH}_2/\text{NH}_3 = 0.5$) and in the 10 km s^{-1} component ($\text{NH}_2/\text{NH}_3 = 0.75$) are consistent with these models.

However, there is evidence that most of the NH_3 in the envelope is located in the shocked component, so that we have to consider shock chemistry as well. The observed column densities and temperatures point to a C-shock as a heating source (Draine 1980). The NH_2 production in this shock is initiated by hydrogen abstraction reactions of N with H_2 to form NH , NH_2 , and NH_3 . The release of atomic hydrogen in this process allows destruction of NH_3 to form NH_2 , so that high abundances of both molecules are maintained. Since all reactions in this chain have high reaction barriers, shock speeds of 25–40 km s^{-1} are needed to make these processes effective (Pineau des Forêts et al. 1993).

Grain surface chemistry has been invoked as an additional source of NH_3 in some regions. The gas-grain models of, e.g., Breukers (1991) and Hasegawa & Herbst (1993), predict NH_3 abundances up to 10^{-5} in the grain mantles but virtually no NH_2 . If this NH_3 is released from the grains, the gas-phase NH_3/NH_2 abundance ratio will temporarily rise to $> 10^3$. Such a scenario very likely applies to the Sgr B2(N) and (M) hot cores but much less to the cold part of the envelope. In the shocked part of the envelope, NH_3 could be released from grain surfaces by means of sputtering (Draine, Roberge, & Dalgarno 1983). If this process takes place, the NH_2/NH_3 ratio in the shocked gas is very low, whereas if grain mantles are absent or no sputtering occurs, the ratio may approach or exceed unity. Since the contributions to the NH_2 column density from the cool and the shocked gas cannot be separated in the intrinsically wide-line Sgr B2 objects, we cannot easily decide which scenario applies to our case. Observations of the NH_2/NH_3 ratio in other objects may help to disentangle the various chemistries.

The authors are indebted to M. Walmsley, T. L. Wilson, D. Lis, P. Bergman, G. Pineau des Forêts, and J. H. Black for useful discussions and for providing information on absorption lines toward Sgr B2 prior to publication. They are grateful to K. Kawaguchi for a list of NH_2 energy levels and line strengths and to the CSO staff for assistance. This work was supported by a PIONIER grant from the Netherlands Organization for Pure Research (NWO) and by NSF contract AST 90-15755 to the California Institute of Technology.

REFERENCES

- Blake, G. A., Keene, J., & Phillips, T. G. 1985, *ApJ*, 295, 501
 Breukers, R. 1991, Ph.D. thesis, Univ. of Leiden
 Burkholder, J. R., Howard, C. J., & McKellar, A. R. W. 1988, *J. Molec. Spectrosc.*, 127, 415
 Charo, A., Sastry, K. V. L. N., Herbst, E., & De Lucia, F. C. 1981, *ApJ*, 244, L111
 Cook, R. L., & De Lucia, F. C. 1971, *Am. J. Phys.*, 39, 1433
 Dalgarno, A., & Black, J. H. 1976, *Rep. Prog. Phys.* 39, 573
 Draine, B. T. 1980, *ApJ*, 241, 1021
 Draine, B. T., Roberge, W. G., & Dalgarno, A. 1983, *ApJ*, 264, 485
 Gardner, F. F., Boes, F., & Winnewisser, G. 1988, *A&A*, 196, 207
 Goldsmith, P. F., Lis, D. C., Hills, R., & Lasenby, J. 1990, *ApJ*, 350, 186
 Greaves, J. S., White, G. J., Ohishi, M., Hasegawa, T., & Sunada, K. 1992, *A&A*, 260, 381
 Herbst, E., & Klemperer, W. 1973, *ApJ*, 185, 505
 Hasegawa, T. I., & Herbst, E. 1993, *ApJ*, in press
 Jacq, T., Walmsley, C. M., Henkel, C., Baudry, A., Mauersberger, R., & Jewell, P. R. 1990, *A&A*, 228, 447
 Keene, J., Blake, G. A., & Phillips, T. G. 1983, *ApJ*, 271, L27
 Langer, W. D., & Graedel, T. E. 1989, *ApJS*, 69, 241
 Le Boulrot, J. 1991, *A&A*, 242, 235
 Lis, D. C., & Goldsmith, P. F. 1989, *ApJ*, 337, 704
 ———. 1991, *ApJ*, 369, 157
 Martín-Pintado, J., de Vicente, P., Wilson, T. L., & Johnston, K. J. 1990, *A&A*, 236, 193
 Meyer, D. M., & Roth, K. 1991, *ApJ*, 376, L49
 Millar, T. J., Rawlings, J. M. C., Bennett, A., Brown, P. D., & Charnley, S. B. 1991, *A&AS*, 87, 585
 Pauls, T. A., Wilson, T. L., Bieging, J. H., & Martin, R. N. 1983, *A&A*, 124, 23
 Phillips, T. G., van Dishoeck, E. F., & Keene, J. 1992, *ApJ*, 399, 533
 Pineau des Forêts, G., Roueff, E., Schilke, P., & Flower, D. R. 1993, *MNRAS*, 262, 915
 Schulz, U., Güsten, R., Serabyn, E., & Walmsley, C. M. 1991, *A&A*, 246, L55
 Storey, J. W. V., Watson, D. M., & Townes, C. H. 1981, *ApJ*, 244, L27
 Sutton, E. C., Blake, G. A., Masson, C. R., & Phillips, T. G. 1985, *ApJS*, 58, 341
 Sutton, E. C., Jaminet, P. A., Danchi, W. C., & Blake, G. A. 1991, *ApJS*, 77, 255
 Thaddeus, P., Kutner, M. L., Penzias, A. A., Wilson, R. W., & Jefferts, K. B. 1972, *ApJ*, 176, L73
 Vogel, S. N., Genzel, R., & Palmer, P. 1987, *ApJ*, 316, 243
 Wilson, T. L., Ruf, K., Walmsley, C. M., Martin, R. N., Pauls, T. A., & Batria, W. 1982, *A&A*, 115, 185